Eur. Phys. J. B **18**, 611–615 (2000)

THE EUROPEAN PHYSICAL JOURNAL B

EDP Sciences

Evolution of the electronic structures of Ni_xSi_y ordered systems: experimental and theoretical investigations

M. Taguchi[1,a], F. Le Normand[2], J. Hommet[2], S. Rey[2], G. Schmerber[3], and J.C. Parlebas[3]

[1] The Abdus Salam International Centre for Theoretical Physics, PO Box 586, 34100 Trieste, Italy
[2] IPCMS-GSI, UMR 7504 CNRS, 23 rue du Loess, 67037 Strasbourg Cedex, France
[3] IPCMS-GEMM, UMR 7504 CNRS, 23 rue du Loess, 67037 Strasbourg Cedex, France

Received 10 July 2000

Abstract. We study the change of the electronic structures of nickel silicides, Ni_3Si and $NiSi_2$, as well as nickel and silicon through the evolution of their valence band X-ray photoelectron spectra (v-XPS) both experimentally and theoretically. The experimental spectra are compared to the total and partial densities of states using tight-binding linear muffin-tin orbital method (TB-LMTO) in the atomic sphere approximation (ASA). Good agreement is found between theory and experiment.

PACS. 71.20.Lp Intermetallic compounds – 79.60.-i Photoemission and photoelectron spectra – 71.20.-b Electron density of states and band structure of crystalline solids

1 Introduction

Many attempts to grow Chemical Vapour Deposition (CVD) diamond on various substrates have been reported, recently [1–4]. Actually there is a need to search for an ideal substrate in order to heteroepitaxially deposit diamond upon it as an electronic active device. Elemental common substrates such as Si or transition metals of the first series (Fe, Co, Ni, Cu ...) do not fulfill all the requirements to conveniently nucleate and grow heteroepitaxial diamond [5]. Among various candidates, the family of transition metal silicides, and especially cubic Ni_3Si and $NiSi_2$, show interesting properties to achieve these requirements [6,7]. Indeed, Ni_3Si (cubic Cu_3Au type structure) and Ni have similar fcc structure, their lattice constants are very close (3.506 Å/3.524 Å) [8] and their lattice mismatches with diamond are very small (1.7%, 1.2%). The difference between them is basically only chemical, due to the incorporation of silicon in the nickel network [9]. On nickel, it is well know that a graphitic layer is rapidly formed which prevents any epitaxial diamond deposition under the CVD process [10], while on a Ni_3Si substrate high-quality diamond could be grown [6] with a clear inhibition of the graphite layer formation. Although $NiSi_2$ (cubic CaF_2 type structure) and diamond have a large mismatch (51%) [11], the incorporation of nickel in the silicon lattice may improve the texturation of diamond films already observed on silicon [12]. Now it is believed that incorporation of nickel in the silicon network will achieve a better matching with diamond. These considerations have motivated us to growth diamond on Ni_xSi_y surfaces, as well as on nickel and silicon substrates in poly- and monocrystalline forms [13].

From a general point of view the electronic properties of contact at the interface (Schottky-type or ohmic barrier) are quite relevant in the performances of future devices. However, in this short paper, we will only focus on the evolution of the electronic structure of (Ni, Si) ordered systems, especially the Ni_3Si and $NiSi_2$ crystal compounds with the corresponding two limiting systems of Ni and Si. More precisely the experimental valence band X-ray photoelectron spectra (v-XPS) are directly compared to our calculated densities of states (DOS) obtained by using a tight-binding-linear-muffin-tin-orbital (TB-LMTO) method. The paper is organized as follows. In Section 2, we recall how the samples were prepared and the v-XPS recorded. Then (Sect. 3) we say a few words on our standard theoretical method to calculate the DOS's. Finally (Sect. 4) we compare and discuss both experimental and theoretical results.

2 Preparation and analyses

A series of bulk Ni_3Si silicides were prepared by arc melting on a water-cooled copper hearth under purified argon atmosphere with a nickel atomic proportion of 77%. In order to remove parasite phases, the samples were annealed in a quartz tube sealed under vacuum for 48 hours at 1173 K. At the end, the alloys were quenched into water.

[a] e-mail: taguchi@ictp.trieste.it

The samples were characterized and checked by conventional X-Ray Diffraction (XRD) and Scanning Electron Microscopy (SEM). All the preparation and characterization details have been reported elsewhere [13]. Nickel and Ni_3Si silicides polycrystalline samples were polished with SiC and diamond powder up to 1μm. Epitaxial $NiSi_2$ (100) silicides were prepared by annealing under Ultra High Vacuum (UHV) of nickel deposited on silicon (100). Temperature and time were respectively 1123 K and 3 hours. The thickness of silicide obtained was 2400 Å. The composition of the silicide layer and the epitaxial relationship with the substrate were checked by Rutherford Back Scattering (RBS) and Transmission Electron Microscopy (TEM). All the samples were ultrasonically rinsed in acetone and methanol for ten minutes before the transfer to an UHV chamber where they were cleaned by different sequences of Ar^+ etching and fast heating. In additional treatment, the silicon sample was etched one minute with fluorhydric acid and rinsed in deionized water prior to the introduction into the UHV chamber. The major part of carbon left by diamond powder and oxygen were then removed. The measurements of the energy distribution of the valence band states have been performed using X-ray photoelectron (XPS). Data were recorded with a VSW-HA150 spectrometer using a monochromatic aluminum anode source at 1486.6 eV. Experimental resolution was about 0.6 eV. The electric contact between the spectrometer and a given sample requires that its Fermi level is equal to the one of the spectrometer. We determined the Fermi level position for each sample by reference with the position measured on the nickel.

3 Theoretical method

$NiSi_2$ crystallises in the fcc CaF_2 (fluorite) structure with a lattice parameter $a_0 = 10.22$ a.u. Whereas Ni_3Si is a $L1_2$ type intermetallic compound and crystallises in the fcc Cu_3Au structure. The lattice parameter of the elemental cube in Ni_3Si is $a_0 = 6.62$ a.u. We also calculated the densities of states (DOS) of fcc Ni structure ($a_0 = 6.65$ a.u.) and semiconducting Si diamond structure ($a_0 = 10.26$ a.u.) for the comparison with Ni_3Si and $NiSi_2$ compounds.

The calculations are based on the density-functional theory within the generalized gradient approximation and Langreth-Mehl-Hu non-local exchange correlation potential [14]. The Kohn-Sham equations are solved self-consistently by using a tight-binding linear-muffin-tin-orbital method (TB-LMTO) in the atomic sphere approximation (ASA) [15,16]. For the k-space integration we used the tetrahedron method [17,18] and an increasing number of k-points, until final convergence was obtained for 165, 286, 165 and 249 k-points in the irreducible Brillouin zone for Ni, Ni_2Si, $NiSi_3$ and Si, respectively.

Figure 1 gives an overview of the total and partial Ni and Si densities of states calculated for Ni, Ni_3Si, $NiSi_2$ and Si. Our results agree well with previous results [19–22]. As well known Si bands have broad structures on both sides of the Fermi energy, while Ni $3d$ bands have a somewhat sharper structure. Furthermore, with increasing formal d occupation of Ni when going from $NiSi_2$ to Ni_3Si, the Fermi level E_F (taken at 0 energy) shifts into the Ni $3d$ bands. In Si, the conduction band below 0 presents three structures. Si $3s$ states are located in the lowest-energy part (about 9–10 eV below E_F). Si $3p$ states are found in the range of 0 to 5 eV below E_F. Mixed states between Si s and p states show up as a peak at 7 eV below E_F. In $NiSi_2$, the main contribution of Ni $3d$ states is found at about 3–4 eV below E_F. Si $3s$ and $3p$ states are located at lower energy (about 5 eV) and Si $3p$ states hybridize with Si $3s$ states so that there are almost no pure Si $3p$ states. In Ni_3Si, Si states are found in the lower-energy part similarly to $NiSi_2$, but now, these states are almost pure Si $3s$ states; the maximum peak of the total DOS is about 1 eV below E_F, with a dominant contribution arising from Ni d states. In Ni metal, as it is well know, the conduction band is almost pure Ni $3d$ states.

4 Comparison between experimental and calculated spectra

The comparison is performed in a simple way, *i.e.* the (convoluted) total DOS is directly compared with measured v-XPS spectra. In order to facilitate a better comparison between theory and experiment, the calculated DOS's have been convoluted both with a Lorentzian and a Gaussian line profiles, which are supposed to simulate both the effects of finite instrumental resolution and lifetime broadening of the excited states. The half width at half-maximum (HWHM) of the Lorentzian as well as Gaussian was chosen to roughly reproduce the width of the experimental structures by 0.2 eV for all compounds under consideration. This procedure, however, neglects the different photoabsorption cross sections of Si and Ni orbitals, which in addition depend on the photon energy. A thorough study of the cross sections of Si and Ni orbitals is beyond the scope of this work.

Figure 2 shows the comparison between v-XPS spectra and convoluted DOS's. For all cases, the v-XPS agrees well with our theoretical results. In addition, the spectrum of the nickel sample is in good agreement with the literature [23]. The so called "6 eV satellite" is observed in v-XPS for Ni metal, while the band structure calculation cannot reproduce this satellite. This satellite has been understood as a contribution of $3d^84s^2$ atomic configuration (see for examples [24,25] and references therein). The valence band of the Si (100) sample displays broad structures at 3.4, 7.4 and 10.1 eV in good agreement with the calculated contributions of the $3p$ states within 1.5–4.5 eV, mixed $3s$ and $3p$ states at 7 eV and $3s$ states around 9.5 eV, respectively [26]. The following additional remarks should be pointed out.

(i) For Ni and Ni_3Si, the v-XPS spectra have almost same spectral shapes, while the density of states for both cases are rather different *i.e.* in the DOS of Ni_3Si,

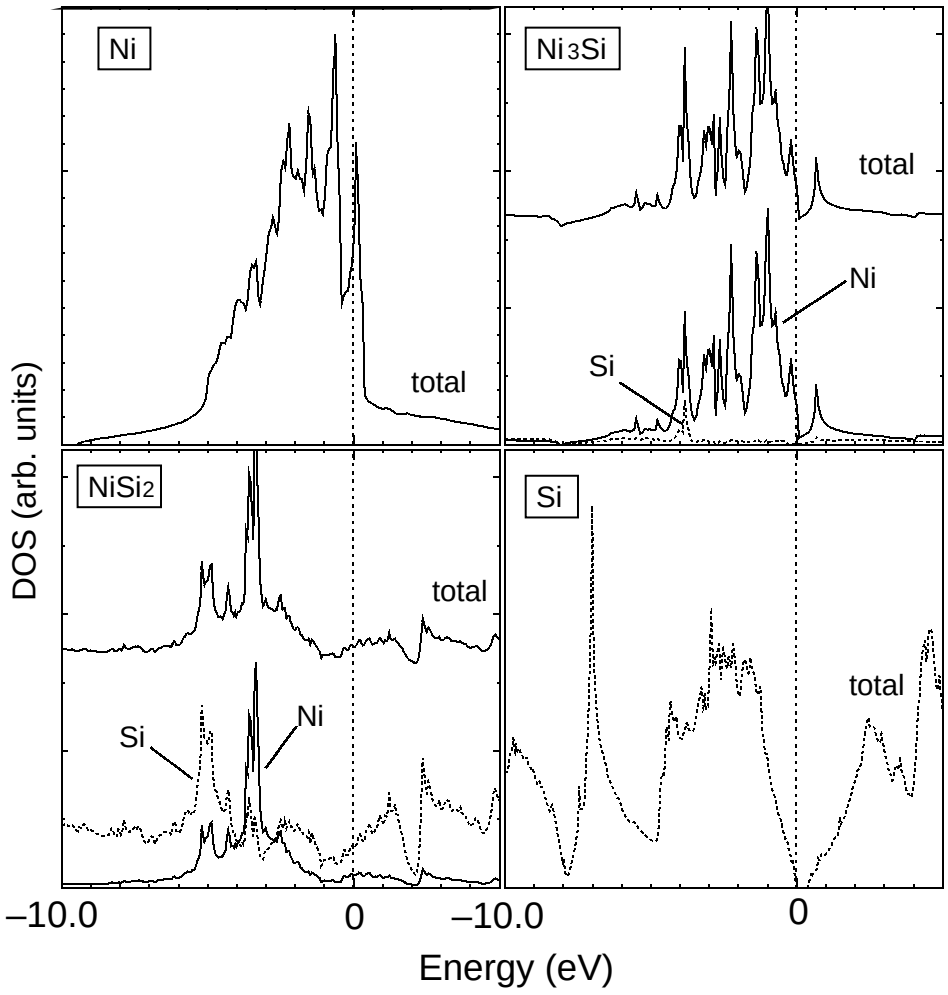

Fig. 1. Total and partial Ni and Si densities of states (DOS) obtained by TB-LMTO method. For Ni_3Si and $NiSi_2$ silicides, the total and partial DOS are shown in the upper and lower parts, respectively. Energies are given relative to the Fermi energy, which in the case of Si was arbitrarily placed at the top of the valence band. The intensity scales for the various systems are different.

the bonding state between Ni d and Si p states are seen at 4 eV below E_F. In both cases, the main peaks of v-XPS spectra arise mainly from Ni $3d$ components. For Ni_3Si compounds, the position of the main peak is rather shifted to the higher binding energy side and the weight of the DOS at E_F (especially Ni $3d$ component) decreases as compared to that of Ni.

(ii) The v-XPS of $NiSi_2$ exhibits completely a different spectral shape. From the density of state, the main peak of v-XPS arises from Ni $3d$ states similarly to Ni and Ni_3Si. The peak position of the main peak, however, is 4 eV below E_F. Moreover, there are two broad hills at each side of the main peak. These hills mainly come from Si components. For $NiSi_2$ compounds, the weight of DOS at E_F decreases even more than for Ni and Ni_3Si and it mainly comes from Si states.

(iii) According to Figure 1, we can see that the Ni $3d$ bands are shifted towards lower energies and their widths are decreased, as we go from Ni to Ni_3Si and $NiSi_2$. These trends are also seen from v-XPS (Fig. 2). The decrease of the Ni $3d$ band width is due to the decrease of hybridization between Ni atoms.

In conclusion, we reported experimental and theoretical results of the valence band X-ray photoelectron spectra for Ni_3Si and $NiSi_2$ compounds in comparison with Ni and Si limiting systems. The total and partial densities of states were calculated using TB-LMTO-ASA methods and compared to the experimental v-XPS spectra. A very good agreement was found between theory and experiment, yielding a unified picture of the evolution of the electronic structure of those Ni_xSi_y ordered systems.

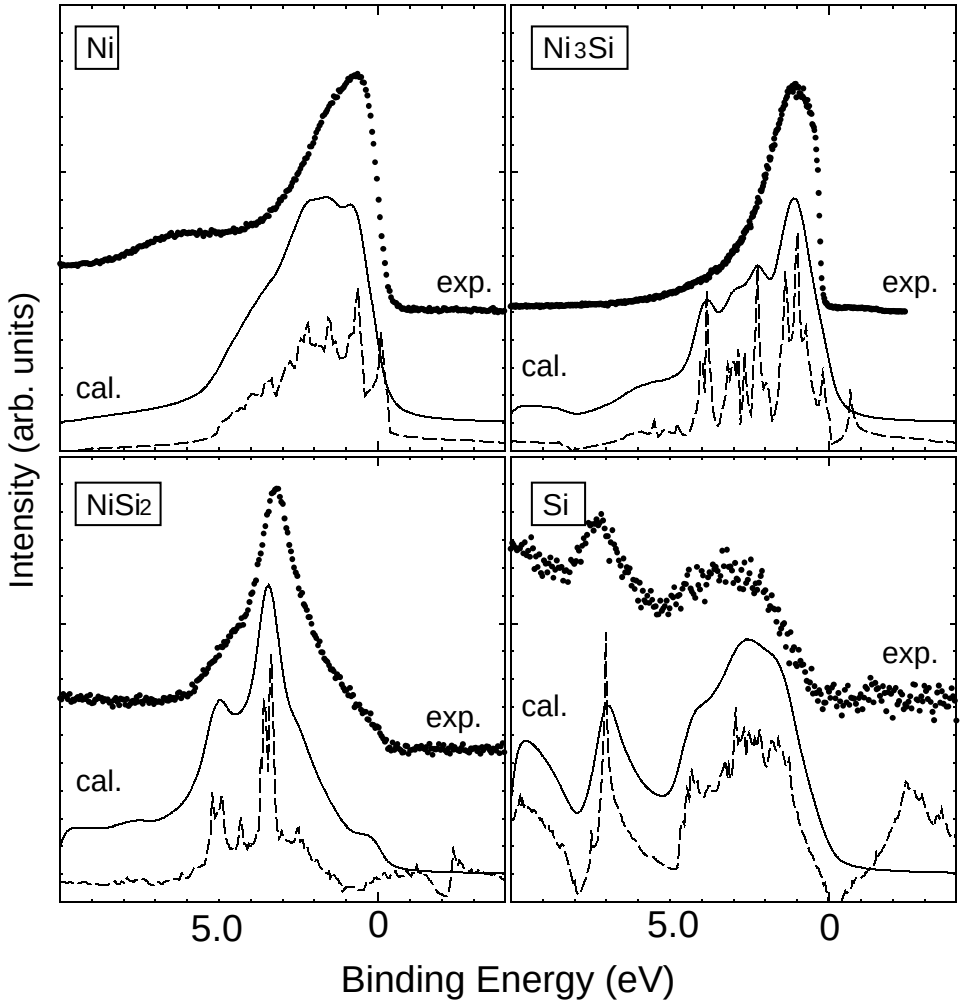

Fig. 2. Comparison of experimental valence band photoemission spectra with the convoluted and calculated density of states. Dotted line is the experimental v-XPS. Full line is the convoluted density of states. Dashed line is total TB-LMTO density of states. Energies are given relative to the Fermi energy, which in the case of Si was arbitrarily placed at the top of the valence band. Of course comparison is only valid for energies below the Fermi level (for filled states).

One of the authors (M. Taguchi) would like to acknowledge gratefully a Visiting Research Fellowship of the Canon Foundation. Dr. J.J. Grob is gratefully acknowledged for providing Ni/Si (100) samples.

References

1. X. Chen, J. Narayan, J. Appl. Phys. **74**, 4168 (1993).
2. L. Demuynck, J.C. Arnault, R. Polini, F. Le Normand, Surf. Sci. **377-379**, 871 (1997).
3. J.C. Arnault, L. Demuynck, C. Speisser, F. Le Normand, Euro. J. Phys. Chem. B **11**, 327 (1999).
4. L. Constant, C. Speisser, F. Le Normand, Surf. Sci. **387**, 28 (1997).
5. H.S. Liu, D.S. Dandy, in *Diamond Chemical Vapor Deposition: Nucleation and early growth stages* (Noyes, Park Ridge, USA, 1995).
6. D.A. Tucker, D.K. Seo, M.H. Whangbo, F.R. Sivazlian, B.R. Stoner, S.P. Bozeman, A.T. Sowers, R.J. Nemanich, J.T. Glass, Surf. Sci. **334**, 179 (1995).
7. J.C. Arnault, B. Lang, F. Le Normand, J. Vac. Sci. Techn. A **16**, 494 (1998).
8. K. Maex, M. Van Rossum, in *Metal Silicides* edited by K. Maex, M. Van Rossum (INSPEC Publication 6, 1995).
9. P. Nash, A. Nash, Bull Alloy Phase Diagrams **8**, 6 (1987).
10. D.N. Belton, S.J. Schmieg, J. Appl. Phys. **66**, 4223 (1989).

11. S.P. Murarka, in *Silicides for VLSI Applications* (Academic Press, 1983).
12. W.J. Zhang, X. Jiang, C.P. Klages, J. Crystal Growth, **171**, 485 (1997).
13. S. Rey, J. Hommet, G. Schmerber, F. Le Normand, J. Cryst. Growth **216**, 225 (2000).
14. D.C. Langreth, M.J. Mehl, Phys. Rev. Lett. **47**, 440 (1981).
15. O.K. Andersen, O. Jepsen, Phys. Rev. Lett. **53**, 2571 (1984).
16. O.K. Andersen, Z. Pawlowska, O. Jepsen, Phys. Rev. B **34**, 5253 (1986).
17. O. Jepsen, O.K. Andersen, Solid State Commun. **9**, 1763 (1971).
18. G. Lehman, M. Taut, Phys. Status. Solidi B **54**, 469 (1972).
19. J.R. Chelikowsky, M.L. Cohen, Phys. Rev. B **14**, 556 (1976).
20. W.R.L. Lambrecht, N.E. Christensen, P. Blöchl, Phys. Rev. B **36**, 2493 (1987).
21. A. Gheorghiu, C. Sénémaud, E. Belin-Ferré, Z. Dankhàzi, L. Magaud-Martinage, D.A. Papaconstantopoulos, J. Phys. Cond. Matt. **8**, 719 (1996).
22. J. Derrien, in *Metal silicides* edited by K. Maex, M. Van Rossum (INSPEC, Stevenage 6, 1995).
23. G.L. Petersson, R. Melander, D.P. Spears, S.B.M. Hagstrom, Phys Rev. B **14**, 4177 (1976).
24. J.C. Parlebas, A. Kotani, S. Tanaka, Prog. Theor. Phys. Suppl. **101**, 271 (1990).
25. S. Hüfner, *Photoelectron Spectroscopy: principle and applications* (Springer-Verlag, 1995).
26. L. Ley, M. Cardona, R.A. Pollak, in *Photoemission in Solids II*, edited by L. Ley, M. Cardona (Springer, Berlin, 1979) p. 56.